Coherent Tunneling and Negative Differential Conductivity in a Graphene/*h*-BN/Graphene Heterostructure

Luis Brey*

Instituto de Ciencia de Materiales de Madrid, CSIC, 28049 Cantoblanco, Spain

(Received 8 May 2014; published 14 July 2014)

We address the tunneling current in a graphene/*h*-BN/graphene heterostructure as a function of the twisting between the crystals. The twisting induces a modulation of the hopping amplitude between the graphene layers that provides the extra momentum necessary to satisfy momentum and energy conservation and to activate coherent tunneling between the graphene electrodes. Conservation rules limit the tunneling to states with wave vectors lying at the conic curves defined by the intersection of two Dirac cones shifted in momentum and energy. There is a critical voltage where the intersection is a straight line, and the joint density of states presents a maximum. This peak in the number of states where both the wave vectors and the energies are matched reflects in a peak in the tunneling current and in a negative differential conductivity.

DOI: 10.1103/PhysRevApplied.2.014003

I. INTRODUCTION

The same techniques used for obtaining graphene layers [1] can also be applied to obtain two-dimensional (2D) crystal structures of highly anisotropic materials such as hexagonal boron nitride (*h*-BN) [2] or transition metal dichalcogenides [3]. Once isolated, atomic layers of different 2D crystals can be reassembled layer by layer to create heterostructures with the designed electrical properties [4]. In this direction, recently, graphene/*h*-BN/graphene [5–7] and graphene-WS_2 [8] heterostructures have been realized and proved as prototype graphene-based field-effect tunneling transistors. At high voltages, the graphene/*h*-BN/graphene structure shows a negative differential conductance [7] that has potential applications for logic devices.

Conservation of energy and momentum prevents finite-voltage coherent tunneling between 2D-electron gases with circular symmetric dispersion. Coherent tunneling occurs only when the Fermi surfaces of the electron gases are closely aligned [9].

In this work, we show that, in graphene/*h*-BN/graphene (G/BN/G) heterostructures, the lattice mismatch between graphene and *h*-BN induces an unavoidable twisting and a spatial modulation of the hopping amplitude between the graphene electrodes. This result translates into a finite-bias coherent-tunneling current between the graphene layers and a negative differential conductivity. We find that, even in the case of perfect crystal arrangement between the graphene layers, the always-present misalignment between graphene and *h*-BN makes possible coherent tunneling between the graphene electrodes. The finite-bias sharp peak and the subsequent negative differential conductivity that occurs in the G/*h*-BN/G heterostructure suggests that these systems, when integrated with a third capacitive terminal gate, could have a large on-off switching ratio and therefore a big potential for high-frequency operation.

II. GEOMETRY AND MODEL

We consider a trilayer structure consisting of top (T) and bottom (B) graphene monolayers separated by L monolayers of *h*-BN. T and B graphene layers are rotated angles θ_T and θ_B, respectively, with respect to the central *h*-BN layers, and they have a lattice parameter mismatch $\delta = 1.8\%$ with *h*-BN. We consider that both graphene layers are incommensurate with the central *h*-BN and there are not crystal deformations associated with the commensurate-incommensurate transitions that could occur at extremely small twisting angles [10–12]. For small twisting angles, the tunneling amplitude between the layers varies over distances much larger than the lattice constant, and electronic states in Dirac points $\mathbf{K}$ and $\mathbf{K}'$ are effectively decoupled. Therefore, we describe each valley separately. Near the Dirac point $\mathbf{K} = (k_D, 0)$ with $k_D = \frac{4\pi}{3a}$, the Hamiltonians for the T and B graphene layers are [13,14]

$$h_{\mathrm{k}}^{T(B)} = \hbar v_F \begin{pmatrix} 0 & k e^{i(\theta_{\mathbf{k}} - \theta_{T(B)})} \\ k e^{-i(\theta_{\mathbf{k}} - \theta_{T(B)})} & 0 \end{pmatrix}, \qquad (1)$$

where $v_F \approx 10^6$ m/s is the graphene Dirac velocity, $\mathbf{k}$ is the momentum measured from the layer's Dirac point, and $\theta_{\mathbf{k}}$ is the angle formed by the momentum with the x axis. Hamiltonian $h_{\mathrm{k}}^{T(B)}$ acts on the amplitude of the wave function on the sublattices A and B of the graphene layer T (B). The electronic structure of each *h*-BN monolayer is described by a gapful Dirac-like Hamiltonian that acts on the B and N atomic basis:

*brey@icmm.csic.es

$$h_{\mathbf{k}}^{\mathrm{BN}} = \begin{pmatrix} \Delta_1 & \hbar v_{\mathrm{BN}} k e^{i\theta_{\mathbf{k}}} \\ \hbar v_{\mathrm{BN}} k e^{-i\theta_{\mathbf{k}}} & -\Delta_2 \end{pmatrix}, \tag{2}$$

where v_{BN} describes the in-plane hopping amplitude between B and N atoms, $\Delta_1 + \Delta_2$ is the energy gap of h-BN, and Δ_1 is the band offset of the conduction band, boronlike, of h-BN with respect to the graphene Dirac point. The different h-BN layers are vertically ordered in an eclipse (AA') way, and the atoms are coupled by a vertical hopping γ_{BN}. This vertical order is a consequence of the bond polarity in h-BN.

Top and bottom graphene layers are coupled with the first and last h-BN layers through the spatially modulated hopping matrices $V(\theta_T, \delta)$ and $V(\theta_B, \delta)$, respectively, that in the low twisting-angle limit ($\theta < 10°$) have the form [15–17]

$$V(\theta, \delta) = \frac{\hat{t}}{3} \sum_{i=1,3} T_i e^{-i\mathbf{q}_i(\theta,\delta)\cdot\mathbf{r}}, \tag{3}$$

with $T_1 = \left(\begin{smallmatrix} 1 & 1 \\ 1 & 1 \end{smallmatrix}\right)$, $T_2 = \left(\begin{smallmatrix} \eta^* & 1 \\ \eta & \eta^* \end{smallmatrix}\right)$, $T_3 = \left(\begin{smallmatrix} \eta & 1 \\ \eta^* & \eta \end{smallmatrix}\right)$, $\hat{t} = \left(\begin{smallmatrix} t_{\mathrm{CB}} & 0 \\ 0 & t_{\mathrm{CN}} \end{smallmatrix}\right)$, and $\eta = e^{i(2\pi/3)}$, t_{CB} and t_{CN} being the C to B and C to N hopping amplitudes, respectively. The hopping matrices T_i do not depend on geometrical factors. All the information on δ and θ is in the $\mathbf{q}_i$'s:

$$\begin{aligned} \mathbf{q}_1(\theta, \delta) &= k_D(\delta, -\theta), \\ \mathbf{q}_2(\theta, \delta) &= k_D\left(-\frac{\sqrt{3}}{2}\theta + \frac{1}{2}\delta, -\frac{1}{2}\theta - \frac{\sqrt{3}}{2}\delta\right), \\ \mathbf{q}_3(\theta, \delta) &= k_D\left(\frac{\sqrt{3}}{2}\theta + \frac{1}{2}\delta, -\frac{1}{2}\theta + \frac{\sqrt{3}}{2}\delta\right). \end{aligned} \tag{4}$$

The three wave vectors $\mathbf{q}_i$ have the same modulus and define a periodic hexagonal modulation of the hopping amplitude. This periodicity describes the spatial distribution of the stacking of the graphene C atoms with the B and N atoms of h-BN.

III. EFFECTIVE HAMILTONIAN

We obtain an effective bilayer graphene Hamiltonian by integrating out the orbital degree of freedom in the h-BN layer:

$$\hat{H}_{\mathbf{k}} = \begin{pmatrix} h^T & 0 \\ 0 & h^B \end{pmatrix} + \begin{pmatrix} 0 & \hat{V} \\ \hat{V}^\dagger & 0 \end{pmatrix}, \tag{5}$$

where

$$\hat{V} = \hat{t} V(\theta_T, \delta) (H_{\mathbf{k}}^{\mathrm{BN}})^{-1} V(-\theta_B, -\delta) \hat{t} \tag{6}$$

and $H_{\mathbf{k}}^{\mathrm{BN}}$ is the Hamiltonian of the L-layer h-BN slab. For wave vectors $\mathbf{k}$, of the order of the separation between the Dirac points of the T and B graphene layers, $|\mathbf{q}_i|$, the diagonal terms Δ_1 and Δ_2 are the leading contributions in the h-BN Hamiltonian $h_{\mathbf{k}}^{\mathrm{BN}}$. For those momenta it is a very good approximation to set $v_{\mathrm{BN}} = 0$ in $h_{\mathbf{k}}^{\mathrm{BN}}$, resulting in the following T to B graphene tunneling modulation:

$$\hat{V} = \frac{1}{9} \sum_{i,j=1,3} \mathcal{T}_{i,j} e^{i\mathbf{G}_{i,j}(\theta_T,\theta_B)\cdot\mathbf{r}} \tag{7}$$

with

$$\mathbf{G}_{i,j}(\theta_T, \theta_B) = \mathbf{q}_i(\theta_T, \delta) + \mathbf{q}_j(-\theta_B, -\delta) \tag{8}$$

and

$$\mathcal{T}_{i,j} = \frac{\gamma_{\mathrm{BN}}^{L-1}}{(\Delta_1\Delta_2)^L} \hat{t} T_i \begin{pmatrix} \Delta_2^L & 0 \\ 0 & \Delta_1^L \end{pmatrix} T_j \hat{t}. \tag{9}$$

The three tunneling processes linking T graphene with h-BN combine with the three connecting h-BN with B graphene. This results in nine Fourier components of the tunneling modulation between T and B graphene layers. The three *diagonal* wave vectors $\{\mathbf{G}_{ii}\}$ have a modulus $G_{\mathrm{d}} = k_D|\theta_T - \theta_B|$ and vanish when T and B layers are aligned. The six *nondiagonal* transfer momenta have modulus $G_{\mathrm{nd}} = k_D\sqrt{\theta_T^2 + \theta_B^2 + \theta_T\theta_B}$. Therefore, even when the two graphene layers are perfectly aligned, the misalignment with the central h-BN layer makes possible tunneling processes between the graphene electrodes. Note that, because the T and B graphene layers have the same lattice parameter, the wave vectors $\{\mathbf{G}_{ij}\}$ are independent on the graphene/h-BN lattice mismatch δ.

IV. TUNNELING CURRENT IN G/*h*-BN/G HETEROSTRUCTURE

In the presence of an applied voltage V, between the T and B graphene electrodes, the tunneling current can be obtained in the linear response theory with the tunneling term treated as the perturbation [18]:

$$\begin{aligned} I(V) = \frac{e}{\hbar} g_s g_v \sum_{\substack{\mathbf{k},\{i,j\} \\ \alpha,\beta}} |t_{\alpha,\beta}(\mathbf{k}, \mathbf{k} + \mathbf{G}_{ij})|^2 \int_{-\infty}^{+\infty} \frac{d\omega}{2\pi} A_\alpha(\mathbf{k}, \hbar\omega) \\ \times A_\beta(\mathbf{k} + \mathbf{G}_{ij}, \hbar\omega + eV)[n_F(\hbar\omega) - n_F(\hbar\omega + eV)], \end{aligned} \tag{10}$$

where $g_s = 2$ and $g_v = 2$ account for the spin and valley degeneracy, respectively, $\alpha = \pm$ is the band index, $n_F(\epsilon) = \{\exp[(\epsilon - E_F)/k_BT] + 1\}^{-1}$ is the Fermi factor, $A_\alpha(\mathbf{k}, \hbar\omega)$ is the graphene spectral function for band α, and $t_{\alpha,\beta}(\mathbf{k}, \mathbf{k} + \mathbf{G}_{ij})$ is the tunneling matrix element between states in the T and B unperturbed graphene layers:

$$t_{\alpha,\beta}(\mathbf{k},\mathbf{k}+\mathbf{G}_{ij}) = \phi^*_\alpha(\mathbf{k})\mathcal{T}_{i,j}\phi_\beta(\mathbf{k}+\mathbf{G}_{ij}), \qquad (11)$$

$\phi_\alpha(\mathbf{k}) = \frac{1}{\sqrt{2}}\binom{1}{\alpha e^{i\theta_\mathbf{k}}}$ being the Dirac Hamiltonian eigenfunction with momentum $\mathbf{k}$ and energy $\alpha\hbar v_F k$. In the previous expressions, E_F is the Fermi energy of the T and B graphene layers that we consider equally doped. In the one-electron picture, the spectral function should be proportional to a δ function; in our calculations, A_α is approximated by a Lorentzian function centered on the band energy $\alpha\hbar v_F k$ and with a half width at half maximum $\hbar/\tau$. In the calculation, we consider the graphene electrodes to be at zero temperature. This temperature is appropriated because, for typical graphene carrier densities, the Fermi energy is much larger than room temperature.

The tunneling processes corresponding to different transfer wave vectors $\mathbf{G}_{i,j}$ contribute independently to the current, and, because of the circular symmetry of the graphene band structure, their contribution to the current depends only on their modulus $|\mathbf{G}_{i,j}|$. Therefore, the relevant quantities or the tunneling current are the two moduli G_d and G_nd.

Because we are considering small twisting angles, we do not observe any features in the I-V curves associated with commensurability, which may occur [19] between the moiré superlattices that emerge in top $[\mathbf{q}_i(\theta_T,\delta)]$ and bottom $[\mathbf{q}_i(-\theta_B,-\delta)]$ graphene layers due to the coupling with the h-BN central layer.

It is important to note that there is a current between the two graphene layers, because they are rotated with respect to the central h-BN layer. In systems with circular symmetric band structure, only the presence of the unavoidable disorder or phonons makes possible the observation of finite-voltage incoherent tunneling between two 2D-electron gases separated by a barrier. On the contrary, in the trilayer G/BN/G heterostructure, the spatial modulation of the hopping amplitude between T and B layers provides an extra wave vector that make possible the conservation of momentum and energy in the coherent tunneling process.

It is possible to get some insight on the different tunneling contributions by analyzing the momentum and energy conservation, together with the Fermi occupation of the T and B layers. In the linear regime, the conduction is different from zero only if the relation $\hbar v_F|\mathbf{G}_{i,j}| < E_F$ is satisfied. That implies finite conductance for twisting angles inside the regions defined by the relations $\hbar v_F k_D|\theta_T+\theta_B| < E_F$ or $\hbar v_F k_D\sqrt{\theta_T^2+\theta_B^2-\theta_T\theta_B} < E_F$. In general, except for very small twist angles, it is appropriate to assume that both G_nd and G_d are smaller than k_F, and therefore in the linear regime the current is zero.

At finite voltage, energy and momentum conservation defines a curve in reciprocal space for the initial tunneling states in the top layer. In general, these curves are the conic sections defined by the intersection of two Dirac cones shifted a momentum $\mathbf{G}_{i,j}$ and an energy eV. At small voltages, the tunneling connects conduction-band states, and the permitted tunneling wave vectors define a hyperbola. At larger voltages, electrons in the valence band of the top layer can tunnel to the conduction-band states of the bottom layer, and the allowed momentums form an ellipse. Both hyperbola and ellipse lengths increase with the voltage, and the current should increase continuously with voltage. However, there is a critical voltage where the hyperbola transforms to an ellipse adopting the form of a straight segment, see Fig. 1. At this critical voltage $V^c = \hbar v_F|\mathbf{G}_{i,j}|$, the cones intersect along two parallel lines, and there is a spike in the joint density of states that translates to a peak in the tunneling current. This peak is the origin of the negative differential conductivity in this heterostructure.

The states defined by these conic curves are further limited by the Fermi occupation. That imposes a minimum voltage $V^{\min} = \hbar v_F(|\mathbf{G}_{i,j}| - 2k_F)$ for the existence of a tunneling current. The Fermi occupation also constrains the wave vectors of the states that tunnel at V^c to be in the interval $|\mathbf{G}_{i,j}| - k_F < k < k_F$.

V. NUMERICAL RESULTS

A precise description of the tunneling current requires the evaluation of the tunneling matrix elements, Eq. (11), which depends on the numerical values of the tight-binding parameters. We assume transferability of the tight-binding parameters [20], and for the trilayer structure we use the hopping parameters obtained recently for graphene/h-BN from *ab initio* calculations by Jung *et al.* [21]: $\Delta_1 = 3.33$ eV, $\Delta_2 = 1.49$ eV, $t_\mathrm{CB} = 0.432$ eV, and

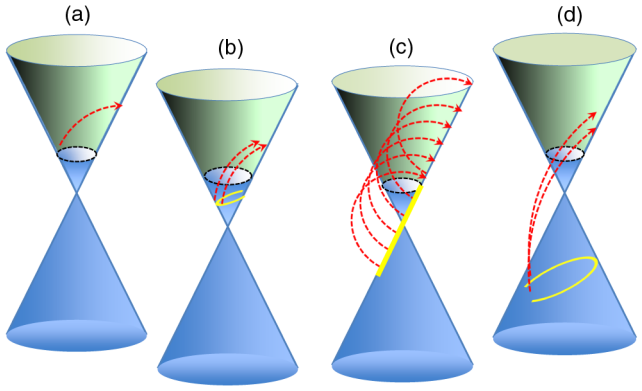

FIG. 1. Schematic representation of tunneling processes occurring in the G/h-BN/G heterostructure. Blue and green regions mark occupied and empty states, respectively. The arrows indicate a tunneling event from the T layer (initial point) to the B layer (end point). These points are shifted in energy by eV. Energy and momentum conservation laws define permitted initial curves in $\mathbf{k}$ space which are plotted in yellow. (a) At the minimum voltage for tunneling, only a point in $\mathbf{k}$ space can tunnel. (b) By increasing the voltage, the conservation curve is a hyperbola that resides in the conduction band. (c) At a critical voltage, the hyperbola collapses in a straight line, and a peak in the joint density of states occurs. (d) At larger voltages, the straight line becomes an ellipse, now residing in the valence band.

$t_{CN} = 0.29$ eV. The separation between T and B graphene layers is ≈0.6 nm, large enough to neglect direct hopping between them. Note that the position of the peak is fixed by the graphene Dirac velocity and the twisting angles and does not depend on particular values of the tight-binding parameters.

In Fig. 2, we plot the current for a G/h-BN/G heterostructure with different twisting angles. We obtain that, at small angles, the tunneling processes associated with the transfer of diagonal momentums $\mathbf{G}_{i,i}$ have a practically null contribution to the current. The main tunneling current is associated with the nondiagonal momentum, and therefore we measure the bias voltages in units of $\hbar v_F G_{\rm nd}$.

In the inset in the upper part of Fig. 2, we show the intraband contribution to the current. The interband contribution is activated at voltage $\hbar v_F(|\mathbf{G}_{\rm nd}| - 2k_F)$ and is zero for voltages larger than $V^c = \hbar v_F |\mathbf{G}_{\rm nd}|$. For $V > V^c$ all the tunneling current has its origin in interband processes. Both inter- and intraband tunneling show a strong peak at this critical voltage. As discussed above, this peak is related to a big increase of the joint density of states occurring at this voltage.

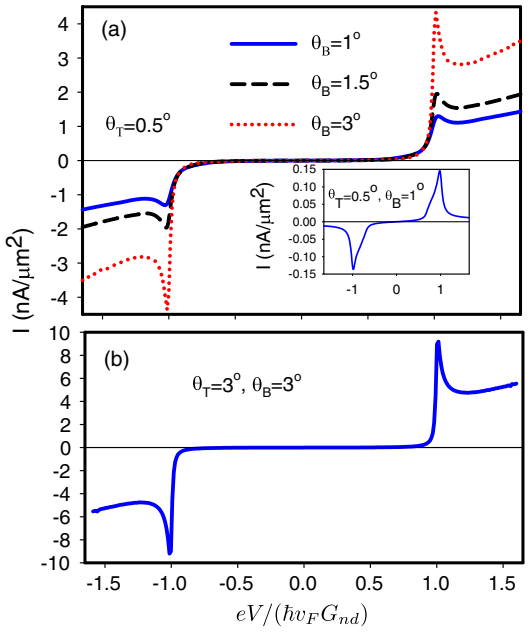

FIG. 2. Nonlinear current for G/h-BN/G. The barrier region consists of a h-BN monolayer. The density of electrons in both layers is $n = 5 \times 10^{12}$ cm^{-2}. In (a), we fix the top-layer twist angle to $\theta_T = 0.5°$ and plot the current for different rotation angles of the bottom layer θ_B. Both angles are measured with respect to the central h-BN layer. In the inset, we show the conduction to conduction ($\alpha = +$ to $\beta = +$) contribution to the current. In (b), both graphene layers are rotated the same angle $\theta_T = \theta_B = 3°$. The peak in the $I(V)$ indicates that coherent tunneling and negative differential conductivity can occur even when both graphene layers are fully aligned, provided there is a twisting with the h-BN layer. In the calculation, we use a quasiparticle lifetime value $\hbar/\tau = 2.5$ meV.

At V^c the interband peak is much stronger than the intraband one. This is because in the intraband tunneling only states with wave vectors in a segment of length k_F contribute the current. However, for interband tunneling the number of wave vectors contributing to tunneling is proportional to $G_{\rm nd} - k_F$. Then, the strong peak in the $I(V)$ curve is due to valence-band-to-conduction-band tunneling processes. In Fig. 2(a), we see that, as the twisting angles become larger, the value of the momentum transfer increases and with it the intensity of the negative differential peak. Finally, the numerical results confirm that the negative differential conductivity peak exists even when both graphene layers are fully aligned (lower panel in Fig. 2).

VI. IN-PLANE MAGNETIC FIELD

A magnetic field applied parallel to the graphene layers affects differently the distinct Fourier components of the interlayer tunneling. Then we expect that the magnetic field splits the negative differential conductivity peak. The experimental observation of this effect would be a definitive indication of the coherent nature of the tunneling.

The magnetic field $\mathbf{B}_\parallel = B_\parallel(\cos\beta, \sin\beta, 0)$ is described in the Landau gauge: $\mathbf{A} = B_\parallel(\sin\beta z, -\cos\beta z, 0)$. For isolated graphene layers, an in-plane magnetic field shifts the position of the Brillouin zones, and its effect can be canceled by distinct gauge transformation for the two graphene sheets. Thus, in the absence of tunneling the magnetic field has no physical relevance. When electrons can hop between the graphene layers, the motion of the carriers perpendicular to the magnetic field is affected by $\mathbf{B}_\parallel$ [22–24], and the shift in the k space reflects in a shift in the tunneling wave vectors:

$$\mathbf{G}_{i,j} \to \mathbf{G}_{i,j} - \frac{d}{\ell_\parallel^2}(\sin\beta, -\cos\beta), \tag{12}$$

$\ell_\parallel = \sqrt{\hbar c/eB_\parallel}$ being the magnetic length and d the separation between the graphene layers. The modulus of the new wave vectors $\mathbf{G}_{i,j}$ depends both on the magnitude of $B_\parallel$ and on its in-plane orientation.

The position of the peak in the $I(V)$ curve is determined by the modulus of the transfer wave vector. For $B_\parallel = 0$ the six nondiagonal wave vectors have the same modulus $G_{\rm nd}$, and only a peak appears; see Fig. 2. The magnetic field modifies the modulus of the transfer wave vectors, and the peak in the $I(V)$ curve broadens and splits in the presence of $B_\parallel$.

In Fig. 3, we plot the effect of $B_\parallel$ on the $I(V)$ peak, for a particular G/h-BN/G heterostructure. The negative differential peak splits in three clear peaks, corresponding to three different transfer wave vectors. The other three wave vectors produce only small shoulders visible only in derivates of the curve. The intensity and resolution of the peaks depends on the tunneling amplitude, on the

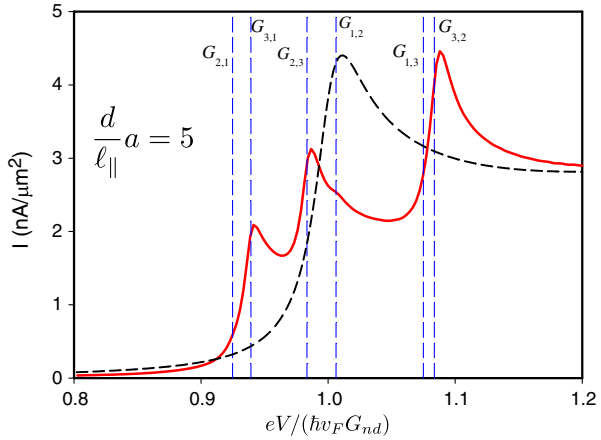

FIG. 3. $I(V)$ curve or a G/h-BN/G structure with twisting angles $\theta_T = -0.5°$ and $\theta_B = 3°$, in the presence of an in-plane magnetic field corresponding to $d\ell_\parallel^{-2}a = 5$, a being the graphene lattice parameter. The barrier region consists of a h-BN monolayer. The density of carriers in both layers is $n = 5 \times 10^{12}$ cm^{-2}. The current for $B_\parallel = 0$ is shown as a black dashed line. Vertical lines indicate the critical voltages corresponding to the different magnetic-field-modified tunneling transfer wave vectors $\mathbf{G}_{i\neq j}$.

strength of $B_\parallel$, on the modulus of the transfer momentum, and on the in-plane orientation of the magnetic field.

In order to observe the effect of the magnetic field, the quantity $d\ell^{-2}$ should be comparable to the value of the modulus of the momentum transfer G_{nd}. This can be achieved by increasing the number of h-BN layers or using a very strong magnetic field. The results presented in Fig. 3 correspond to just one h-BN layer, and the magnetic field corresponding to $d\ell_\parallel^{-2}a = 5$ is of the order of 80 T. By increasing the number of h-BN layers, the separation between graphene layers becomes larger, and the magnetic field required for observing the splitting of the peak should be more accessible.

We note that recent field effect tunneling [6] and negative differential conductance [7] experiments in G/h-BN/G heterostructures have been explained by assuming disorder-induced momentum conservation relaxation and therefore noncoherent tunneling. Also, recently, Feenstra *et al.* [25,26] considered the tunneling between n- and p-doped graphene layers separated by a dielectric barrier. That work applied the transfer Hamiltonian formalism to model the tunneling between misoriented graphene layers, and the information on the dielectric crystal structure is neglected.

In summary, we have studied the tunneling current between two graphene layers separated by a h-BN layer. The twisting of the layers induces a spatial modulation of the hopping amplitude between the graphene electrodes that provide extra wave vectors to the tunneling process. These extra momenta make possible the conservation of energy and momentum and activate coherent tunneling. Because of the Dirac-like linear dispersion of graphene, the wave vectors that conserve energy and momentum in the tunneling process can be defined as the intersection of two Dirac cones shifted in momentum and energy. At a critical voltage, the intersection conic curves collapse in a straight segment, and there is a strong peak in the joint density of states and in the tunneling current.

ACKNOWLEDGMENTS

This work has been partially supported by MEC-Spain under Grant No. FIS2012-33521. L. B. thanks C. Tejedor for a critical reading of the manuscript.

Note added.—We recently learned about the experimental work of K. Novoselov *et al.*, where possible signatures of negative differential conductance and coherent tunneling in G/***h***-BN/G heterostructures were reported [27].

[1] K. S. Novoselov, A. K. Geim, S. V. Morozov, D. Jiang, Y. Zhang, S. V. Dubonos, I. V. Gregorieva, and A. A. Firsov, Electric field effect in atomically thin carbon films, Science **306**, 666 (2004).

[2] C. R. Dean, A. F. Young, I. Meric, C. Lee, L. Wang, S. Sorgenfrei, K. Watanabe, T. Taniguchi, P. Kim, K. L. Shepard, and J. Hone, Boron nitride substrates for high-quality graphene electronics, Nat. Nanotechnol. **5**, 722 (2010).

[3] Kin Fai Mak, Changgu Lee, James Hone, Jie Shan, and Tony F. Heinz, Atomically thin: MoS_2: A new direct-gap semiconductor, Phys. Rev. Lett. **105**, 136805 (2010).

[4] A. K. Geim and I. V. Grigorieva, Van der Waals heterostructures, Nature (London) **499**, 419 (2013).

[5] Gwan-Hyoung Lee, Young-Jun Yu, Changgu Lee, Cory Dean, Kenneth L. Shepard, Philip Kim, and James Hone, Electron tunneling through atomically flat and ultrathin hexagonal boron nitride, Appl. Phys. Lett. **99**, 243114 (2011).

[6] L. Britnell, R. V. Gorbachev, R. Jalil, B. D. Belle, F. Schedin, A. Mishchenko, T. Georgiou, M. I. Katsnelson, L. Eaves, S. V. Morozov, N. M. R. Peres, J. Leist, A. K. Geim, K. S. Novoselov, and L. A. Ponomarenko, Field-effect tunneling transistor based on vertical graphene heterostructures, Science **335**, 947 (2012).

[7] L. Britnell, R. V. Gorbachev, A. K. Geim, L. A. Ponomarenko, A. Mishchenko, M. T. Greenaway, T. M. Fromhold, K. S. Novoselov, and L. Eaves, Resonant tunnelling and negative differential conductance in graphene transistors, Nat. Commun. **4**, 1794 (2013).

[8] T. Georgiou, R. Jalil, B. D. Belle, L. Britnell, R. V. Gorbachev, S. V. Morozov, Y.-J. Kim, A. Gholinia, S. J. Haigh, O. Makarovsky, L. Eaves, L. A. Ponomarenko, A. K. Geim, K. S. Novoselov, and A. Mishchenko, Vertical field-effect transistor based on graphene-WS_2 heterostructures for flexible and transparent electronics, Nat. Nanotechnol. **8**, 100 (2013).

[9] J. P. Eisenstein, L. N. Pfeiffer, and K. W. West, Field induced resonant tunneling between parallel two dimensional electron systems, Appl. Phys. Lett. **58**, 1497 (1991).
[10] C. R. Woods, L. Britnell, A. Eckmann, R. S. Ma, J. C. Lu, H. M. Guo, X. Lin, G. L. Yu, Y. Cao, R. V. Gorbachev, A. V. Kretinin, J. Park, L. A. Ponomarenko, M. I. Katsnelson, Yu. N. Gornostyrev, K. Watanabe, T. Taniguchi, C. Casiraghi, H.-J. Gao, A. K. Geim, and K. S. Novoselov, Commensurate-incommensurate transition in graphene on hexagonal boron nitride, Nat. Phys. **10**, 451 (2014).
[11] J. Jung, A. DaSilva, A. H. MacDonald, and S. Adam, Origin of band gaps in graphene on hexagonal boron nitride, arXiv:1403.0496.
[12] P. San-Jose, Á. Gutiérrez, M. Sturla, and F. Guinea, Spontaneous strains and gap in graphene on boron nitride, arXiv:1404.7777.
[13] Tsuneya Ando, Theory of electronic states and transport in carbon nanotubes, J. Phys. Soc. Jpn. **74**, 777 (2005).
[14] A. H. Castro Neto, F. Guinea, N. M. R. Peres, K. S. Novoselov, and A. K. Geim, The electronic properties of graphene, Rev. Mod. Phys. **81**, 109 (2009).
[15] J. M. B. Lopes dos Santos, N. M. R. Peres, and A. H. Castro Neto, Graphene bilayer with a twist: Electronic structure, Phys. Rev. Lett. **99**, 256802 (2007).
[16] Rafi Bistritzer and Allan H. MacDonald, Moire bands in twisted double-layer graphene, Proc. Natl. Acad. Sci. U.S.A. **108**, 12233 (2011).
[17] M. Kindermann, Bruno Uchoa, and D. L. Miller, Zero-energy modes and gate-tunable gap in graphene on hexagonal boron nitride, Phys. Rev. B **86**, 115415 (2012).
[18] G. D. Mahan, *Many Particle Physics* (Plenum, New York, 1981).
[19] R. Bistritzer and A. H. MacDonald, Transport between twisted graphene layers, Phys. Rev. B **81**, 245412 (2010).
[20] Walter A. Harrison, *Electronic Structure and the Properties of Solids* (Dover, New York, 1989).
[21] J. Jung, A. Raoux, Z. Qiao, and A. H. MacDonald, *Ab initio* theory of moiré superlattice bands in layered two-dimensional materials, Phys. Rev. B **89**, 205414 (2014).
[22] R. K. Hayden, D. K. Maude, L. Eaves, E. C. Valadares, M. Henini, F. W. Sheard, O. H. Hughes, J. C. Portal, and L. Cury, Probing the hole dispersion curves of a quantum well using resonant magnetotunneling spectroscopy, Phys. Rev. Lett. **66**, 1749 (1991).
[23] L. Brey, G. Platero, and C. Tejedor, Effect of a high transverse magnetic field on the tunneling through barriers between semiconductors and superlattices, Phys. Rev. B **38**, 9649 (1988).
[24] V. I. Fal'ko and S. V. Meshkov, On resonant oscillations in current-voltage characteristics of double-barrier heterostructures, Semicond. Sci. Technol. **6**, 196 (1991).
[25] R. M. Feenstra, Debdeep Jena, and Gong Gu, Single-particle tunneling in doped graphene-insulator-graphene junctions, J. Appl. Phys. **111**, 043711 (2012).
[26] G. Fiori, S. Bruzzone, and G. Iannaccone, Very large current modulation in vertical heterostructure graphene/hBN transistors, IEEE Trans. Electron Devices **60**, 268 (2013).
[27] K. Novoselov *et al.*, Graphene, other 2D atomic crystals and their heterostructures, Bull. Am. Phys. Soc. **59**, T39 (2014).